Microstrip Filter Design Using Direct EM Field Simulation

John W. Bandler, *Fellow, IEEE,* Radoslaw M. Biernacki, *Senior Member, IEEE,* Shao Hua Chen, *Member, IEEE,* Daniel G. Swanson, Jr., *Senior Member, IEEE,* and Shen Ye, *Member, IEEE*

***Abstract*— For the first time, we present minimax filter design with electromagnetic (EM) simulations driven directly by a gradient-based optimizer. Challenges of efficiency, discretization of geometrical dimensions, and continuity of optimization variables are overcome by a three-stage attack: 1) efficient on-line response interpolation with respect to geometrical dimensions of microstrip structures simulated with fixed grid sizes; 2) smooth and accurate gradient evaluation for use in conjunction with the proposed interpolation; and 3) storing the results of expensive EM simulations in a dynamically updated database. Simulation of a lowpass microstrip filter illustrates the conventional use of EM simulation for design validation. Design optimization of a double folded stub bandstop filter and of a millimeter-wave 26–40 GHz interdigital capacitor bandpass microstrip filter illustrates the new technique.**

I. INTRODUCTION

We present results of microwave filter design with accurate electromagnetic (EM) simulations driven by a minimax gradient-based optimizer. We exploit recent advances [1]–[5] in EM simulation which give the designer the opportunity to accurately simulate passive circuit components, in particular microstrip structures [2]. However, we go far beyond the prevailing use of stand-alone EM simulators, namely, validation of designs obtained through less accurate techniques.

EM simulators, although computationally intensive, are regarded as accurate at microwave frequencies, extending the validity of the models to higher frequencies, including millimeter-wave frequencies, and they cover wider parameter ranges [2]. EM simulators, whether stand-alone or incorporated into software frameworks, will not realize their full potential to the designer (whose task is to obtain the best parameter values satisfying design specifications) unless they are optimizer-driven to automatically adjust designable parameters.

Manuscript received July 27, 1993; revised January 12, 1994. This work was supported in part by Optimization Systems Associates Inc. and in part by the Natural Sciences and Engineering Research Council of Canada under Grants OGP0007239, OGP0042444, and STR0117819 and through an Industrial Research Fellowship to S. Ye.

J. W. Bandler, R. M. Biernacki, and S. H. Chen are with Optimization Systems Associates Inc., Dundas, Ont., Canada L9H 5E7, and the Simulation Optimization Systems Research Laboratory, Department of Electrical and Computer Engineering, McMaster University, Hamilton, Ont., Canada L8S 4L7.

D. G. Swanson, Jr., is with Watkins-Johnson Company, Palo Alto, CA 94304-1204 USA.

S. Ye was with Optimization Systems Associates Inc., Dundas, Ont., Canada L9H 5E7. He is now with Com Dev Ltd., Cambridge, Ont., Canada N1R 7H6.

IEEE Log Number 9402409.

Design optimization tools are widely available (e.g., [6]), typically in conjunction with analytical, heuristic models of microstrip structures developed in recent years. Consequently, designers, using such tools, try to generate designs in the form of either equivalent circuits, or physical parameters based on approximate models. Using an EM simulator, designers currently validate and improve their designs by manual adjustments. The need for direct design optimization with accurate field simulation is clear.

The feasibility of optimizing passive structures using EM simulation has already been shown in [3], [4]. Our paper addresses several challenges arising when EM simulations are to be put directly into the optimization loop. We consider the advantages of on-line EM simulations (performed on request) as opposed to up-front simulations, as in Jansen's look-up table approach. The requirement of circuit responses for continuously varying optimization variables must be reconciled with inherent discretization of geometrical parameters present in numerical EM simulations. Finally, the requirement of providing the optimizer with smooth and accurate gradient information must be given serious attention. We effectively deal with all these problems, contributing a new dimension to this subject.

The results presented in this paper have been obtained using Empipe™ [7], an interface between OSA90/hope™ [8] and ***em***™ [5]. On-line interpolation is applied to geometrical dimensions of microstrip structures to provide for continuity of optimization variables in the presence of fixed grid sizes in the EM simulations. The results of the EM simulations are stored in a database and can be retrieved if, during optimization, the same on-the-grid points need to be resimulated.

The proposed geometrical interpolation has been tested on a number of microstrip structures. The conventional use of EM simulation for design validation is illustrated by comparing the results of ***em*** [5] simulation and the corresponding measurements of a lowpass microstrip filter. Design optimization of a double folded stub filter for bandstop applications and of a millimeter-wave 26–40 GHz interdigital capacitor microstrip bandpass filter demonstrates the new technique.

Minimax design optimization is briefly reviewed in Section II. Section III includes our theory of geometrical interpolation, and Section IV contains a derivation of gradient expressions for use in conjunction with geometrical interpolation. Storing the results of expensive EM simulations in a database and issues of updating the database are discussed in Section V. Finally, Sections VI–VIII describe our experiments.

II. Minimax Design Optimization

Frequency-domain design of microwave filters involves design specifications imposed on the responses (S parameters, return loss, insertion loss, etc.). In order to formulate an objective function for design optimization, the filter is simulated at a given point (vector) of designable (optimization) variables $\boldsymbol{\phi}$ and at the same frequency points at which the upper (S_{uj}) and/or lower (S_{lj}) specifications are given. The corresponding responses, denoted by $R_j(\boldsymbol{\phi})$, determine the error vector $\boldsymbol{e}(\boldsymbol{\phi})$ as

$$\boldsymbol{e}(\boldsymbol{\phi}) = [e_1(\boldsymbol{\phi}) \quad e_2(\boldsymbol{\phi}) \cdots e_M(\boldsymbol{\phi})]^T \tag{1}$$

where the individual errors $e_j(\boldsymbol{\phi})$ are of the form

$$e_j(\boldsymbol{\phi}) = R_j(\boldsymbol{\phi}) - S_{uj} \tag{2}$$

or

$$e_j(\boldsymbol{\phi}) = S_{lj} - R_j(\boldsymbol{\phi}) \tag{3}$$

and M is the total number of errors. A negative error value indicates that the corresponding specification is satisfied. For positive error values, the corresponding specifications are violated. All the errors $e_j(\boldsymbol{\phi})$ are combined into a single objective function to be minimized. Minimax design optimization is defined as

$$\underset{\boldsymbol{\phi}}{\text{minimize}} \left(\max_j \left(e_j(\boldsymbol{\phi}) \right) \right). \tag{4}$$

Effective minimax optimization requires a dedicated optimizer, such as [9], and accurate gradients of individual errors with respect to the optimization variables $\boldsymbol{\phi}$.

III. Geometrical Interpolation

The vector $\boldsymbol{\psi}$ of all geometrical parameters (structure lengths, widths, spacings, etc.) of a planar microstrip structure can be written as

$$\boldsymbol{\psi} = [\boldsymbol{\psi}_{opt}^T(\boldsymbol{\phi}) \quad \boldsymbol{\psi}_{fix}^T]^T \tag{5}$$

where the vector $\boldsymbol{\psi}_{opt}(\boldsymbol{\phi})$ contains designable geometrical parameters which are either directly the optimization variables or are functions of the optimization variables $\boldsymbol{\phi}$, and the vector $\boldsymbol{\psi}_{fix}$ contains fixed geometrical parameters. It is important to realize that each component of $\boldsymbol{\psi}$ belongs to one of the three physical orientations (x, y, or z) and, therefore, the vector $\boldsymbol{\psi}$ can be rearranged as

$$\boldsymbol{\psi} = [\boldsymbol{\psi}^{xT} \quad \boldsymbol{\psi}^{yT} \quad \boldsymbol{\psi}^{zT}]^T. \tag{6}$$

Numerical EM simulation is performed for discretized values of the geometrical parameters $\boldsymbol{\psi}$. Let the discretization matrix $\boldsymbol{\delta}$ be defined by the grid sizes Δx_i, Δy_i, and Δz_i as

$$\begin{aligned}\boldsymbol{\delta} &= \text{diag}\,\{\delta_i\} \\ &= \text{diag}\,\{\Delta x_1,\, \Delta x_2, \cdots, \Delta y_1,\, \Delta y_2, \cdots, \Delta z_1,\, \Delta z_2, \cdots\}.\end{aligned} \tag{7}$$

A specific EM simulator may allow only one grid size for each orientation while others may provide the flexibility of independent Δx_i, Δy_i, and Δz_i for different parameters of the same x, y, or z orientation. For uniform discretization in each direction $\Delta x_i = \Delta x$, $\Delta y_i = \Delta y$, and $\Delta z_i = \Delta z$.

Before invoking EM simulation for a given $\boldsymbol{\psi}$, it is necessary to find "the nearest" point (vector) on the grid, denoted by $\boldsymbol{\psi}^c$, which we call the *center base point*. We define it by the equation

$$\boldsymbol{\psi} = \boldsymbol{\psi}^c + \boldsymbol{\delta\theta} \tag{8}$$

subject to suitable conditions imposed on $\boldsymbol{\theta}$ to precisely define the term "the nearest." For example, the conditions on $\boldsymbol{\theta}$ can be chosen as

$$-0.5 \le \theta_i < 0.5, \qquad i = 1, 2, \cdots, n \tag{9}$$

or as

$$0 \le \theta_i < 1, \qquad i = 1, 2, \cdots, n \tag{10}$$

where n is the total number of geometrical parameters and $\boldsymbol{\theta}$ is the relative deviation of $\boldsymbol{\psi}$ from the center base point. $\boldsymbol{\psi}^c$ and $\boldsymbol{\theta}$ can be easily determined using the "floor" function as

$$\psi_i^c = |[\psi_i/\delta_i + 0.5]|\delta_i \quad \text{or} \quad \psi_i^c = |[\psi_i/\delta_i]|\delta_i \tag{11}$$

for (9) or (10), respectively, and

$$\theta_i = (\psi_i - \psi_i^c)/\delta_i. \tag{12}$$

If $\boldsymbol{\theta} \neq \mathbf{0}$, the point is off-the-grid and we use interpolation to determine each response $R(\boldsymbol{\psi})$. We drop the subscript j and take (5) into account in expressing $R_j(\boldsymbol{\phi})$. We consider the class of interpolation problems where the interpolating function can be expressed as a linear combination of some *fundamental interpolating functions* in terms of deviations with respect to the center base point. Let $\boldsymbol{f}(\boldsymbol{\delta\theta})$ be the vector of fundamental interpolating functions

$$\boldsymbol{f}(\boldsymbol{\delta\theta}) = [f_1(\boldsymbol{\delta\theta}) \quad f_2(\boldsymbol{\delta\theta}) \cdots f_K(\boldsymbol{\delta\theta})]^T. \tag{13}$$

We want to find a vector

$$\boldsymbol{a} = [a_1 \quad a_2 \cdots a_K]^T \tag{14}$$

such that

$$R(\boldsymbol{\psi}) - R(\boldsymbol{\psi}^c) = \boldsymbol{f}^T(\boldsymbol{\delta\theta})\boldsymbol{a} \tag{15}$$

holds exactly at K selected *base points*. Once $\boldsymbol{a}$ is determined, (15) will be used to interpolate the response elsewhere in a suitably defined *interpolation region* around the center base point $\boldsymbol{\psi}^c$. The *interpolation base* B in the space of geometrical parameters is a set of grid points defined as

$$B = \{\boldsymbol{\psi}^c\} \cup \{\boldsymbol{\psi} | \boldsymbol{\psi} = \boldsymbol{\psi}^c + \boldsymbol{S\delta\eta},\, \boldsymbol{\eta} \in B^\eta\} \tag{16}$$

where

$$B^\eta = \{\boldsymbol{\eta}^j | \boldsymbol{\eta}^j \in I^n,\, \boldsymbol{\eta}^j \neq \mathbf{0},\, \boldsymbol{\eta}^i \neq \boldsymbol{\eta}^j, i, j = 1, 2, \cdots, K\} \tag{17}$$

is a set of predefined integer vectors called *relative interpolation base*, and

$$\boldsymbol{S} = \text{diag}\,\{s_i\},$$

where

$$s_i = \begin{cases} 1 & \text{if } \psi_i \text{ is a nonsymmetric parameter} \\ 2 & \text{if } \psi_i \text{ is a symmetric parameter.} \end{cases} \quad (18)$$

The symmetry matrix $\boldsymbol{S}$ accounts for double grid size increments for parameters whose dimensions are modified by extending or contracting both ends simultaneously.

The interpolation base B is used as the set of base points $\boldsymbol{\psi}^c$ and $\boldsymbol{\psi}^{bj}$, $j = 1, 2, \cdots, K$, at which EM simulation is invoked to evaluate the corresponding set of responses $R_{EM}(\boldsymbol{\psi}^c)$, $R_{EM}(\boldsymbol{\psi}^{b_1}), \cdots, R_{EM}(\boldsymbol{\psi}^{bK})$. From (15), we formulate a set of K linear equations

$$[\Delta R_{EM}(\boldsymbol{\psi}^{b_1})\, \Delta R_{EM}(\boldsymbol{\psi}^{b_2}) \cdots \Delta R_{EM}(\boldsymbol{\psi}^{bK})]^T = [\boldsymbol{f}(\boldsymbol{S\delta\eta}^1)\, \boldsymbol{f}(\boldsymbol{S\delta\eta}^2) \cdots \boldsymbol{f}(\boldsymbol{S\delta\eta}^K)]^T \boldsymbol{a} \quad (19)$$

where $\Delta R_{EM}(\boldsymbol{\psi}^{bj}) = R_{EM}(\boldsymbol{\psi}^{bj}) - R_{EM}(\boldsymbol{\psi}^c)$. More concisely,

$$\Delta \boldsymbol{R}_{EM}(B) = \boldsymbol{F}(\boldsymbol{S\delta}, B^{\eta})\boldsymbol{a}. \quad (20)$$

By solving (20), we determine the vector $\boldsymbol{a}$ of interpolation coefficients as

$$\boldsymbol{a} = \boldsymbol{F}^{-1}(\boldsymbol{S\delta}, B^{\eta})\Delta \boldsymbol{R}_{EM}(B) \quad (21)$$

which, after substituting into (15), gives

$$R(\boldsymbol{\psi}) = R_{EM}(\boldsymbol{\psi}^c) + \boldsymbol{f}^T(\boldsymbol{\delta\theta})\boldsymbol{F}^{-1}(\boldsymbol{S\delta}, B^{\eta})\Delta \boldsymbol{R}_{EM}(B). \quad (22)$$

Equation (22) provides the response values for the off-the-grid points. Note that the matrix $\boldsymbol{F}(\boldsymbol{S\delta}, B^{\eta})$ in (20) must be invertible. This, however, depends only on the selection of the fundamental interpolating functions and the relative interpolation base B^{η} and can be determined prior to all calculations. It is also independent of the center base point, so the same formulas are involved as the variables move during optimization.

IV. Gradient Estimation

To facilitate the use of an efficient and robust dedicated gradient minimax optimizer, we need to provide the gradients of the errors (2) and (3), or the gradients of $R_j(\boldsymbol{\phi})$. From (5), we can determine

$$\nabla_{\phi} R_j(\boldsymbol{\phi}) = \nabla_{\phi}\boldsymbol{\psi}^T(\boldsymbol{\phi})\nabla_{\psi}R(\boldsymbol{\psi}). \quad (23)$$

The first factor on the right-hand side of (23) is readily available since the mapping (5), as an integral part of the problem formulation, is known. The second factor on the right-hand side of (23) must be determined using EM simulations.

During optimization, it is very likely that the gradient will be requested at off-the-grid points. As discussed in Section III, the responses at off-the-grid points are determined by interpolation. It is, therefore, most appropriate from the optimizer's point of view to provide the gradient of the interpolating function, i.e., the function that is actually returned to the optimizer. This is fortunate since that gradient can be analytically derived from the fundamental interpolating functions. From (22), we get

$$\nabla_{\psi} R(\boldsymbol{\psi}) = \nabla_{\delta\theta}\boldsymbol{f}^T(\boldsymbol{\delta\theta})\boldsymbol{F}^{-1}(\boldsymbol{S\delta}, B^{\eta})\Delta \boldsymbol{R}_{EM}(B). \quad (24)$$

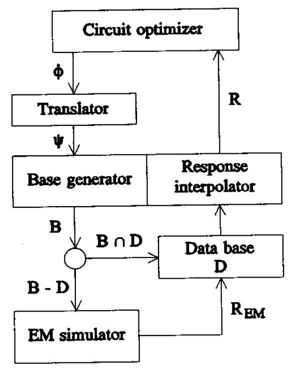

Fig. 1. Flow diagram illustrating the interconnection between a circuit optimizer and a numerical EM simulator.

Equation (24) gives accurate gradient information for the optimizer in a simple, straightforward, and efficient manner. Note that $\boldsymbol{F}^{-1}(\boldsymbol{S\delta}, B^{\eta})$ and $\Delta \boldsymbol{R}(B)$ are already available from response interpolation.

Some optimizers may request perturbed simulation in the vicinity of the nominal point $\boldsymbol{\phi}^0$, say at $\boldsymbol{\phi}^{pert}$, in order to estimate the gradient by perturbation, instead of using the gradient at $\boldsymbol{\phi}^0$ directly. In such cases, using (22) at $\boldsymbol{\phi}^{pert}$ may provide a different result from (24) unless the fundamental interpolating functions are linear. As the exact gradient (24) is available, a modified response at $\boldsymbol{\phi}^{pert}$ can be easily evaluated from the linearized interpolating function at $\boldsymbol{\phi}^0$ as

$$R(\boldsymbol{\psi}^{pert}) = R_{EM}(\boldsymbol{\psi}^c) + [\boldsymbol{f}^T(\boldsymbol{\delta\theta}^0) + (\boldsymbol{\psi}^{pert} - \boldsymbol{\psi}^0)^T \nabla_{\delta\theta}\boldsymbol{f}^T(\boldsymbol{\delta\theta}^0)] \cdot \boldsymbol{F}^{-1}(\boldsymbol{S\delta}, B^{\eta})\Delta \boldsymbol{R}_{EM}(B) \quad (25)$$

where $\boldsymbol{\psi}^0$, $\boldsymbol{\theta}^0$, and $\boldsymbol{\psi}^{pert}$ are determined from $\boldsymbol{\phi}^0$ and $\boldsymbol{\phi}^{pert}$, respectively. This formula, when used in gradient estimation by perturbation, will produce the same result as (24).

V. Updating the Database of Simulated Results

In order to efficiently utilize the results of EM simulations and to reduce their number, we have considered two levels of control. First, interpolation is invoked only when necessary, i.e., if a specific θ_i is zero we exclude the corresponding base point from the interpolation base. To be able to implement such a scheme, the fundamental interpolating functions must be appropriately devised. Second, a database D of base points and the corresponding responses obtained from exact EM simulations is stored and accessed when necessary (see Fig. 1). Each time EM simulation is requested, the corresponding interpolation base B is generated and checked against the existing database. Actual EM simulation is invoked only for the base points not present in the database $(B - D)$. Results for the base points already present in the database $(B \cap D)$ are simply retrieved from D and used for interpolation.

Updating the database D is a separate issue. Between the two extremes: 1) all simulated results are saved, and 2) only results for the latest interpolation base are saved, many schemes can be adopted depending on such factors as required

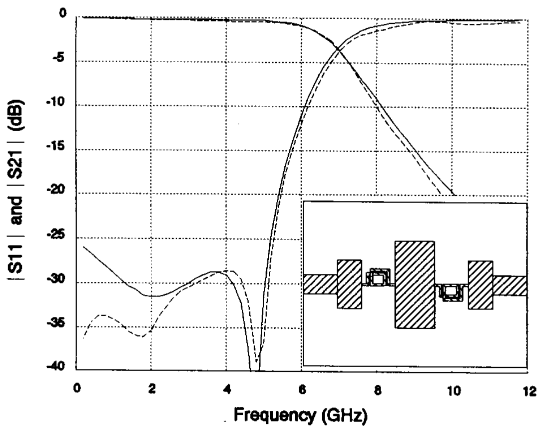

Fig. 2. EM simulation and measurements of the lowpass filter shown in the insert: simulated (——) and measured (- - -) $|S_{11}|$ and $|S_{21}|$. The thickness and dielectric constant of the substrate are 25 mils and 9.8, respectively.

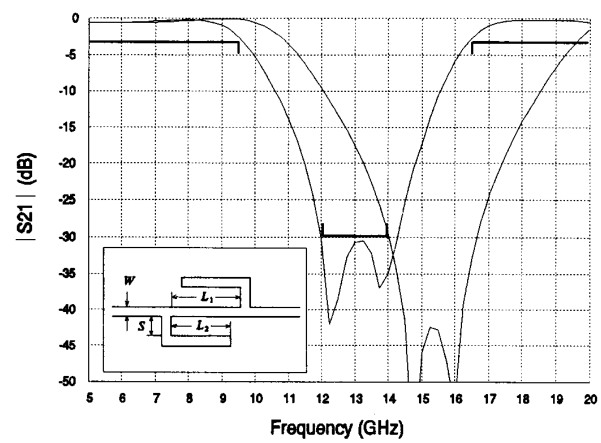

Fig. 3. $|S_{21}|$ before and after optimization for the double folded stub bandstop filter structure shown in the insert.

memory, access time, repeated simulations, etc. In any case, however, it is worthwhile to remember the current (active) interpolation base. This is particularly useful in (25), even if the perturbed point falls outside the interpolation region.

VI. Experimental Validation of a Microstrip Filter Design

A conventional, and until now state-of-the-art, use of EM simulation for design validation is illustrated by comparing measurements and EM simulation of the lowpass microstrip filter shown in the insert in Fig. 2. The filter was designed by first synthesizing an LC prototype, and then designing the corresponding microstrip components to match those of the prototype.

The filter was built on a 25-mil-thick alumina substrate with a relative dielectric constant of 9.8. The rectangular inductors, utilizing air bridges with vias, were made of 2-mil-wide lines with 1-mil gaps and occupied a total area of 19×16 mils. The center capacitor had dimensions of 50×115 mils and the end capacitors 35×74 mils (the value of 75 mils was used for simulation). The measurements on the filter were taken at frequencies from 0.2 to 11.8 GHz with a step of 0.2 GHz. The measured $|S_{11}|$ and $|S_{21}|$ versus frequency are shown in Fig. 2, together with the corresponding plots obtained by electromagnetic simulation using ***em*** [5].

On a Sun SPARCstation 2, simulation was carried out for the same frequency range from 0.2 to 11.8 GHz with a step of 0.2 GHz. For simulation, the whole structure was partitioned into individual components—capacitors and inductors—the latter including the connecting transmission lines. Because of symmetry, only one inductor and one end capacitor were simulated. Additional pieces of transmission lines were added for each component and de-embedded for better accuracy and to account for discontinuities at both sides of each capacitor.

The simulation times were approximately 100 s for the inductor, 10 s for the center capacitor, and 8 s for the end capacitor, all per one frequency point. The resulting S parameters of the individual components were then combined to determine the S parameters of the overall filter. The results give a very good approximation of filter behavior in all critical areas, in particular around the cutoff frequency. The discrepancies between measured and simulated $|S_{11}|$ at very low frequencies may be due to numerical problems in the EM simulation that becomes apparent when vias are electrically very short.

VII. Design of Double Folded Stub Microstrip Structure

A double folded stub microstrip structure for bandstop filter applications, shown in the insert in Fig. 3, may substantially reduce the filter area while achieving the same goal as the conventional double stub structure [10]. The symmetrical double folded stub can be described by 4 parameters: width (W), spacing (S), and two lengths (L_1 and L_2). The input and output reference planes are located at the stubs.

We used minimax optimization to move the center frequency of the stopband from 15 to 13 GHz. W was fixed at 4.8 mils, and L_1, L_2, and S were optimization variables with the starting values given by [10]. Design specifications were taken as

$$|S_{21}| > -3\,\text{dB} \qquad \text{for } f < 9.5 \text{ GHz and } f > 16.5 \text{ GHz}$$

$$|S_{21}| < -30 \text{ dB} \qquad \text{for } 12 \text{ GHz} < f < 14 \text{ GHz}.$$

The substrate thickness and the relative dielectric constant were 5 mils and 9.9, respectively.

Optimization was carried out in two steps. First, we applied identical $\Delta x = \Delta y = 2.4$ mils grid size in both x and y directions. Then the grid size was reduced to $\Delta x = \Delta y = 1.6$ mils for fine resolution. The values of the optimization variables before and after optimization are reported in Table I. Fig. 3 shows $|S_{21}|$ in decibels versus frequency before and after optimization, with the center frequency clearly moved to 13 GHz as desired.

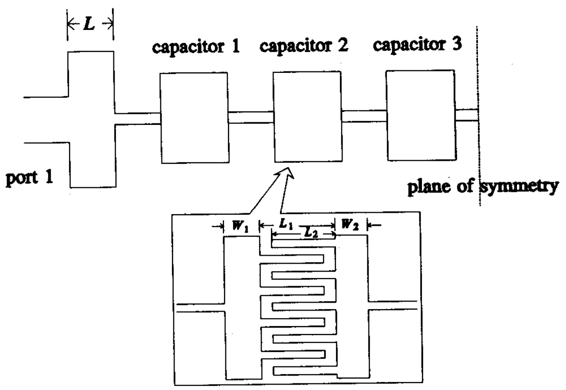

Fig. 4. The 26–40 GHz millimeter-wave bandpass filter. The dielectric constant is 2.25. Substrate thickness and shielding height are 10 and 120 mils, respectively. The optimization variables include L, and L_1, L_2, W_1, W_2 for each capacitor, totaling 13.

TABLE I
PARAMETER VALUES FOR THE DOUBLE FOLDED STUB BEFORE AND AFTER OPTIMIZATION

Parameter	Before optimization (mil)	After optimization (mil)
L_1	74.0	91.82
L_2	62.0	84.71
S	13.0	4.80

VIII. DESIGN OF A MILLIMETER-WAVE MICROSTRIP FILTER

A 26–40 GHz millimeter-wave bandpass filter [11] was built on a 10-mil-thick substrate with relative dielectric constant of 2.25. The filter, shown in Fig. 4, utilized high impedance microstrip lines and interdigital capacitors to realize inductances and capacitances of a synthesized lumped ladder circuit. The filter was designed to satisfy the specifications

$$|S_{11}| < -20 \text{ dB}$$

$$|S_{21}| > -0.04 \text{ dB}$$

for 26 GHz $< f <$ 40 GHz. The original microstrip design was determined by manually matching each element of the lumped prototype at the center frequency using ***em*** [5]. However, when the filter was simulated by ***em*** in the whole frequency range, the results exhibited significant discrepancies with respect to the prototype. It necessitated a tedious series of manual interpolations and made a satisfactory design very difficult to achieve. The filter was then built and measured [11].

The redesign of the bandpass filter was carried out using ***em*** [5] driven by our minimax gradient optimizer. There was a total of 13 designable parameters including the distance between the patches L_1, the finger length L_2, and two patch widths W_1 and W_2 for each of the three interdigital capacitors, and the length L of the end capacitor, as shown in Fig. 4. The finger width and spacing for all capacitors were held constant at 2.0 mils. The transmission lines between the capacitors were fixed at the originally designed values. The second half of the circuit, to the right of the plane of symmetry, is assumed identical to the first half, so it contains no additional variables.

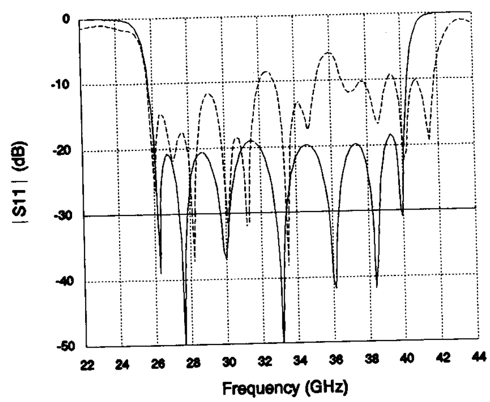

(a)

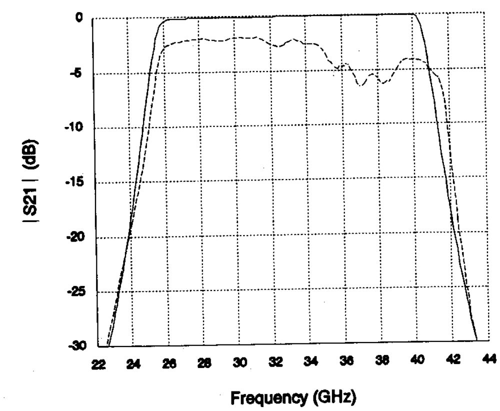

(b)

Fig. 5. The 26–40 GHz millimeter-wave bandpass filter after minimax optimization and fabrication. All the optimization variables have been rounded to 0.1 mil resolution. Simulated (——) and measured (- - -): (a) $|S_{11}|$, and (b) $|S_{21}|$.

A typical minimax equal-ripple response of the filter was achieved after a series of consecutive optimizations with different subsets of optimization variables and frequency points [12]. The filter was then built with the resulting geometrical dimensions rounded to 0.1 mil resolution. Fig. 5 shows the corresponding simulated and measured filter responses: $|S_{11}|$ and $|S_{21}|$. The larger error in the measured results appears to be in the bandwidth which points to analysis of the series capacitors. A grid size of 1.0 mil in both x and y directions was used for the interdigital capacitor simulation. More recent error analysis studies [13] indicate that 6–10 cells across the width of the finger may be needed to reduce the error in computed capacitance to below 1.0%. This filter is also surprisingly sensitive to the impedance and phase velocity of the series transmission lines. The same convergence issues discussed for the interdigital capacitors also apply to the series transmission lines. Experimentally, we found it very difficult to hold ±0.1 mil tolerances in the 0.23-mil-thick metallization.

IX. Conclusions

For the first time, we have presented a comprehensive approach to microwave filter design which exploits accurate electromagnetic field simulations driven directly by a powerful gradient-based minimax optimizer. The benefits of electromagnetic simulations are thus significantly extended. Our approach, illustrated by simulation of two microstrip structures and the minimax design of two filters, paves the way for direct use of field theory-based simulation in practical optimization-driven microwave circuit design.

Acknowledgment

The authors thank Dr. J. C. Rautio of Sonnet Software, Inc., Liverpool, NY. His initiatives, encouragement, and help substantially facilitated this timely and important work.

References

[1] J. C. Rautio and R. F. Harrington, "An electromagnetic time-harmonic analysis of arbitrary microstrip circuits," *IEEE Trans. Microwave Theory Tech.*, vol. 35, pp. 726–730, 1987.

[2] T. Itoh, Ed., *Numerical Techniques for Microwave and Millimeter-Wave Passive Structures.* New York: Wiley, 1989.

[3] R. H. Jansen and P. Pogatzki, "A hierarchically structured, comprehensive CAD system for field theory-based linear and nonlinear MIC/MMIC design," in *1992 2nd Int. Workshop German IEEE MTT/AP Joint Chapter Integrated Nonlinear Microwave Millimeterwave Circuits Dig.*, Duisburg, Germany, 1992, pp. 333–341.

[4] *LINMIC+/N Version 3.0*, Jansen Microwave, Bürohaus am See, Am Brüll 17, D-4030 Ratingen 1, Germany, 1992.

[5] *Em User's Manual*, Sonnet Software, Inc., 135 Old Cove Road, Suite 203, Liverpool, NY 13090-3774, May 1992.

[6] J. W. Bandler and S. H. Chen, "Circuit optimization: the state of the art," *IEEE Trans. Microwave Theory Tech.*, vol. 36, pp. 424–443, 1988.

[7] *Empipe™ Version 1.1 User's Manual*, Optimization Systems Associates Inc., P.O. Box 8083, Dundas, Ont., Canada L9H 5E7, 1993.

[8] *OSA90/hope™ Version 2.5 User's Manual*, Optimization Systems Associates Inc., P.O. Box 8083, Dundas, Ont., Canada L9H 5E7, 1993.

[9] J. W. Bandler, W. Kellermann, and K. Madsen, "A superlinearly convergent minimax algorithm for microwave circuit design," *IEEE Trans. Microwave Theory Tech.*, vol. MTT-33, pp. 1519–1530, 1985.

[10] J. C. Rautio, Sonnet Software, Inc., 135 Old Cove Road, Suite 203, Liverpool, NY 13090-3774, private communication, 1992.

[11] D. G. Swanson, Jr., Watkins-Johnson Company, 3333 Hillview Avenue, Stanford Research Park, Palo Alto, CA 94304-1204, private communication, 1992.

[12] J. W. Bandler, S. Ye, R. M. Biernacki, S. H. Chen, and D. G. Swanson, Jr., "Minimax microstrip filter design using direct EM field simulation," in *IEEE MTT-S Int. Microwave Symp. Dig.*, Atlanta, GA, 1993, pp. 889–892.

[13] J. C. Rautio *et al.*, "Critical issues in experimental validation," presented at the Workshop WSMK, IEEE MTT-S Int. Microwave Symp., Atlanta, GA, 1993.

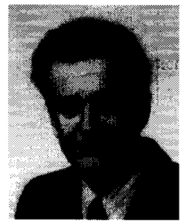

John W. Bandler (S'66–M'66–SM'74–F'78) was born in Jerusalem, on November 9, 1941. He studied at Imperial College of Science and Technology, London, England, from 1960 to 1966. He received the B.Sc.(Eng.), Ph.D., and D.Sc.(Eng.) degrees from the University of London, London, England, in 1963, 1967, and 1976, respectively.

He joined Mullard Research Laboratories, Redhill, Surrey, England, in 1966. From 1967 to 1969 he was a Postdoctorate Fellow and Sessional Lecturer at the University of Manitoba, Winnipeg, Canada. He joined McMaster University, Hamilton, Canada, in 1969, where he is currently Professor of Electrical and Computer Engineering. He has served as Chairman of the Department of Electrical Engineering and Dean of the Faculty of Engineering. He currently directs research in the Simulation Optimization Systems Research Laboratory. He is President of Optimization Systems Associates Inc. (OSA), which he founded in 1983. OSA introduced the CAE systems RoMPE™ in 1988, HarPE™ in 1989, OSA90™ and OSA90/hope™ in 1991, and Empipe™ in 1992. He is President of Bandler Research Inc., which he founded in 1989. He contributed to *Modern Filter Theory and Design* (New York: Wiley-Interscience, 1973) and to *Analog Methods for Computer-Aided Analysis and Diagnosis* (New York: Marcel Dekker, 1988). He has published more than 260 papers, four of which appear in *Computer-Aided Filter Design* (New York: IEEE Press, 1973), one in each of *Microwave Integrated Circuits* (Norwood, MA: Artech House, 1975), *Low-Noise Microwave Transistors and Amplifiers* (New York: IEEE Press, 1981), *Microwave Integrated Circuits*, 2nd ed. (Norwood, MA: Artech House, 1985), *Statistical Design of Integrated Circuits* (New York: IEEE Press, 1987), and *Analog Fault Diagnosis* (New York: IEEE Press, 1987).

Dr. Bandler was an Associate Editor of the IEEE Transactions on Microwave Theory and Techniques (1969–1974), Guest Editor of the Special Issue of the IEEE Transactions on Microwave Theory and Techniques on Computer-Oriented Microwave Practices (March 1974), and Guest Co-Editor with R. H. Jansen of the Special Issue of the IEEE Transactions on Microwave Theory and Techniques on Process-Oriented Microwave CAD and Modeling (July 1992). He joined the Editorial Boards of the *International Journal of Numerical Modelling* in 1987, and the *International Journal of Microwave and Millimeterwave Computer-Aided Engineering* in 1989. He is a Fellow of the Royal Society of Canada, a Fellow of the Institution of Electrical Engineers (Great Britain), a member of the Association of Professional Engineers of the Province of Ontario (Canada), and a Member of the Electromagnetics Academy.

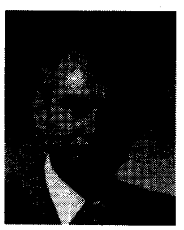

Radoslaw M. Biernacki (M'85–SM'86) was born in Warsaw, Poland. He received the Ph.D. degree from the Technical University of Warsaw, Warsaw, Poland, in 1976.

He became a Research and Teaching Assistant in 1969 and an Assistant Professor in 1976 at the Institute of Electronics Fundamentals, Technical University of Warsaw, Warsaw, Poland. From 1978 to 1980 he was on leave with the Research Group on Simulation, Optimization and Control and with the Department of Electrical and Computer Engineering, McMaster University, Hamilton, Canada, as a Postdoctorate Fellow. From 1984 to 1986 he was a Visiting Associate Professor at Texas A&M University, College Station, TX. He joined Optimization Systems Associates Inc., Dundas, Ont., Canada, in 1986, where he is currently Vice President Research and Development. At OSA he has been involved in the development of commercial CAE software systems HarPE™, OSA90™, and OSA90/hope™, and related research on parameter extraction, statistical device modeling, simulation and optimization, including yield-driven design, of linear and nonlinear microwave circuits. Since 1988 he has been a Professor (part time) in the Department of Electrical and Computer Engineering, McMaster University, Hamilton, Canada. His research interests include system theory, optimization and numerical methods, computer-aided design of integrated circuits and control systems. He has more than 80 publications.

Dr. Biernacki has been the recipient of several prizes for his research and teaching activities.

Shao Hua Chen (S'84–M'88) was born in Swatow, Guangdong, China, on September 27, 1957. He received the B.S.(Eng.) degree from the South China Institute of Technology, Guangzhou, China, in 1982 and the Ph.D. degree in electrical engineering from McMaster University, Hamilton, Canada in 1987.

From July 1982 to August 1983, he was a Teaching Assistant in the Department of Automation at the South China Institute of Technology. He was a graduate student in the Department of Electrical and Computer Engineering at McMaster University from 1983 to 1987, during which time he was awarded an Ontario Graduate Scholarship for two academic years. He joined Optimization Systems Associates Inc., Dundas, Ont., Canada, in 1987 and engaged in commercial CAD software development. He has made major contributions to the development of the CAE systems HarPE^{TM} and OSA90/hope^{TM}. Currently he is working as a Research Engineer in the Simulation Optimization Systems ResearchLaboratory at McMaster University. His professional interests include optimization theory and implementation, CAD software architecture, device modeling, statistical simulation, circuit design centering, sensitivity analysis, computer graphics, and user interfaces.

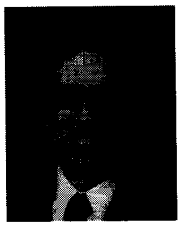

Daniel G. Swanson, Jr. (S'74–M'78–SM'91) received the B.S.E.E. degree from the University of Illinois in 1976 and the M.S.E.E. degree from the University of Michigan in 1978.

In 1978 he joined Narda Microwave, where he developed a 6–18 GHz low-noise amplifier, an 8–10 GHz low-noise amplifier, and a de-embedding system for S-parameter device characterization. In 1980 he was with the Wiltron Company designing YIG tuned oscillators for use in microwave sweepers. He also developed a broad-band load-pull system for optimization of output power. In 1983 he joined a startup company, Iridian Microwave, where he was responsible for the dielectric resonator oscillator product line. In 1984 he joined Avantek Inc., where he developed thin-film microwave filters, software for filter design, and a low-frequency broad-band GaAs MMIC amplifier. In 1989 he joined Watkins-Johnson Company where he is Staff Scientist. His current work includes thin-film filter design and the application of electromagnetic field solvers to microwave component design.

Mr. Swanson served as an officer in the Santa Clara Valley Chapter of the MTT-S from 1985 to 1989. He is presently serving as MTT-S AdCom Treasurer. He is a member of Eta Kappa Nu.

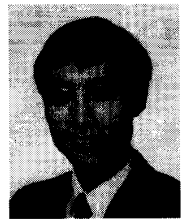

Shen Ye (S'88–M'92) was born in Shanghai, China, in 1957. He received the B.Eng. and M.Eng. degrees from Shanghai University of Technology, Shanghai, China, in 1982 and 1984, respectively, and the Ph.D. degree from McMaster University, Hamilton, Canada, in 1991, all in electrical engineering.

From 1984 to 1986 he was a Teaching and Research Assistant in the Department of Electrical Engineering, Shanghai University of Technology. He joined the Simulation Optimization Systems Research Laboratory and the Department of Electrical and Computer Engineering, McMaster University as a graduate student in 1986. He held an Ontario Graduate Scholarship for the academic year 1989–1990. In 1991 he was awarded an Industrial Research Fellowship from the Natural Sciences and Engineering Research Council of Canada and was a Research Engineer with Optimization Systems Associates Inc., Dundas, Ont., Canada, from 1991 to 1993. He contributed substantially to the design and implementation of Empipe^{TM}. In 1993 he joined Com Dev Ltd., Cambridge, Ont., Canada, where he is a Design Engineer. His professional interests include general CAD software design, simulation and optimization techniques, design and optimization of microwave circuits, device modeling, parameter extraction, and statistical circuit design.